9522–9533 *Nucleic Acids Research, 2012, Vol. 40, No. 19* *Published online 16 August 2012*
doi:10.1093/nar/gks767

The arginine methyltransferase PRMT6 regulates cell proliferation and senescence through transcriptional repression of tumor suppressor genes

Claudia Stein, Stefanie Riedl, Diana Rüthnick, René Reiner Nötzold and Uta-Maria Bauer*

Institute for Molecular Biology and Tumor Research (IMT), University of Marburg, Emil-Mannkopff-Strasse 2, 35032 Marburg, Germany

Received June 5, 2012; Revised July 13, 2012; Accepted July 20, 2012

ABSTRACT

The protein arginine methyltransferase 6 (PRMT6) is a coregulator of gene expression and executes its repressing as well as activating function by asymmetric dimethylation of histone H3 at R2 (H3 R2me2a). Given that elevated expression levels of PRMT6 have been reported in various cancer types, we explore here its role in cell proliferation and senescence. We find that knockdown of PRMT6 results in proliferation defects of transformed as well as non-transformed cells, causes G1-phase arrest and induces senescence. This phenotype is accompanied by transcriptional upregulation of important cell cycle regulators, most prominently the cyclin-dependent kinase (CDK) inhibitor gene p21 ($p21^{CIP1/WAF1}$, CDKN1A) and p16 ($p16^{INK4A}$, CDKN2A). Chromatin immunoprecipitation analysis reveals that the p21 gene is a direct target of PRMT6 and the corresponding histone mark H3 R2me2a. Using a cell model of oncogene-induced senescence (OIS), in which p21 is an essential activator of the senescent phenotype, we show that PRMT6 expression declines upon induction of senescence and conversely p21 gene expression increases. Moreover, overexpression of PRMT6 leads to reduced levels of OIS. These findings indicate that the transcriptional repressor activity of PRMT6 facilitates cell proliferation and blocks senescence by regulation of tumor suppressor genes and that this might contribute to the oncogenic capacity of PRMT6.

INTRODUCTION

Arginine methylation is an evolutionary conserved posttranslational modification, which is catalyzed by protein arginine methyltransferases (PRMTs). In mammals, these enzymes constitute a family of nine members (PRMT1-9), which share a conserved catalytic domain and perform mono- and dimethylation of the terminal guanidino nitrogens of arginine residues (1,2). Dimethylation can either be asymmetric or symmetric. A subgroup of PRMTs methylates histones as well as non-histone chromatin proteins and thereby regulates chromatin-dependent processes. Like other chromatin-modifying enzymes, PRMTs function as transcriptional coregulators and contribute either to activation or repression of gene expression (3). The enzymes themselves do not possess the capability to directly bind DNA and are recruited via interaction with transcription factors to their genomic target sites. The transcriptional functions involve PRMTs in important cellular processes, such as the regulation of cell proliferation, differentiation and apoptosis (1).

The family member PRMT6 conducts asymmetric dimethylation and prefers monomethylated arginines as substrates (4–6). In agreement with its predominant nuclear localization, the enzyme is implicated in the regulation of nuclear processes, such as DNA repair and gene expression. PRMT6 influences nucleotide excision repair by modifying the DNA polymerase β and thereby enhances the processivity of the polymerase (7). PRMT6 also plays a role in transcriptional regulation by inhibition of viral transcription and replication through methylation of the HIV transactivator protein Tat (8). Further, PRMT6 possesses histone methyltransferase activity and modifies the four core histones with histone H3

*To whom correspondence should be addressed. Tel: +49 6421 2865325; Fax: +49 6421 2865196; Email: bauer@imt.uni-marburg.de
Present address:
Claudia Stein, Novartis Institutes for Biomedical Research (NIBR), Developmental & Molecular Pathways (DMP), Basel, Switzerland.

The authors wish it to be known that, in their opinion, the first two authors should be regarded as joint First Authors.

asymmetrically dimethylated at arginine 2 (H3 R2me2a) being the major *in vivo* methylation site (6,9,10). The H3 R2me2a modification contributes to transcriptional repression of HoxA genes, Myc target genes and Thrombospondin-1 (TSP1), whereas it participates in transcriptional activation of the cyclin D1 gene specifically in response to DNA-damage stimulation. H3 R2me2a accomplishes these gene regulatory functions by antagonizing H3 K4 trimethylation (H3 K4me3) and subsequent effector binding to the H3 K4me3 mark (6,9–11). In addition, it was found that PRMT6 together with PRMT4 acts as a synergistic coactivator in nuclear hormone receptor-regulated gene expression; however, the relevance of its activity toward H3 R2me2a was not addressed in this context (12).

Recent reports revealed that PRMT6 is overexpressed in several cancer types, such as breast, cervix, bladder, prostate and lung cancer, indicating that elevated levels of the enzyme might be beneficial for tumor growth and progression (13). In agreement with this, depletion of PRMT6 in a subset of tumor cell lines suppresses viability and growth (12,13). Although deregulated PRMT6 expression likely leads to an aberrant transcriptional response, which might contribute to neoplastic transformation, the relevant downstream targets of PRMT6 have so far not been described. Only the TSP1 gene, which was recently identified as a PRMT6 repressed target and which is an inhibitor of angiogenesis and cell migration, hints at a potential function of PRMT6 in tumor progression and metastasis (11).

In an attempt to define the role of PRMT6 in proliferation control, we show here that depletion of PRMT6 reduces the rate of cell devision, leads to cell cycle arrest and senescence. We identified the cyclin-dependent kinase (CDK) inhibitor gene p21 ($p21^{CIP1/WAF1}$, CDKN1A) as an important and direct downstream target of this pro-proliferative activity of PRMT6 and the corresponding histone modification H3 R2me2a. Expression of PRMT6 and p21 was found to be inversely regulated in a cell model of oncogene-induced senescence (OIS), in which p21 was revealed as a significant activator of the senescent phenotype. Moreover, overexpression of PRMT6 in this model of OIS led to reduced levels of senescence. Our findings unravel that the transcriptional repressor activity of PRMT6 is required for cell proliferation and prevents senescence by repressing p21 gene expression. Thereby, PRMT6 might contribute to an unlimited proliferation and evasion of senescence during cellular transformation.

MATERIALS AND METHODS

Cell lines and antibodies

Telomerase (hTERT)-immortalized TIG3-T cells (which express the ecotropic receptor) (14), hTERT-immortalized TIG3 BRAF-estrogen receptor (ER) cells [which express a 4-hydroxytamoxifen (4-OHT) inducible oncogenic BRAF-ER fusion] (15,16), U2OS and Phoenix cells were maintained in DMEM supplemented with 10% fetal calf serum (Gibco/BRL) at 37°C and 5% CO_2. TIG3 BRAF-ER cells were treated every 2 days with 200 nM 4-OHT (Sigma) for the indicated time periods. The following antibodies were employed: affinity-purified anti-PRMT6 rabbit serum was produced using GST-tagged proteins corresponding to amino acids 1–375 of human PRMT6, anti-p21 from Santa Cruz (sc-469), anti-p27 from Cell Signaling (3686), anti-p16 from Santa Cruz (sc-65224), anti-cyclin A2 from Santa Cruz (sc-751), anti-H3 R2me2a (asymmetric) from Millipore (07-585), anti-H3 from Abcam (ab1791), anti-CDK2 from Santa Cruz (sc-163), anti-βTubulin from Millipore (MAB3408) and rabbit immunoglobulin G (IgG) from Sigma.

Short interfering RNAs, short hairpin RNAs, transfection and retroviral infection

Short interfering RNA (siRNA) oligonucleotide duplexes were obtained from Dharmacon, Eurogentec or Sigma for targeting the human PRMT6 and p21 transcripts, respectively, or control (non-targeting) siRNAs. The following siRNA sequences were employed (sense strand indicated): siPRMT6_1 5′-GAGCAAGACACGGACGUUU-3′; siPRMT6_2 5′-GCAAGACACGGACGUUUCA-3′; siPRMT6_3 5′-GGAGGGAGAGUGACUUCAU-3′; siPRMT6_4 5′-GACGUUUCAGGAGAGAUCA-3′; siPRMT6_5 5′-CGGAACAGGUGGAUGCCAU-3′; sip21 (pool of three sequences) 5′-CGAUGGAACUUC GACUUUG-3′, 5′-GCGAUGGAACUUCGACUUU-3′ and 5′-GAUGGAACUUCGACUUUGU-3′; siLuci 5′-G AUUAUGUCCGGUUAUGUA-3′; siNon 5′-AUGAAC GUGAAUUGCUCAA-3′; siScr 5′-CAUAAGCUGAGA UACUUCA-3′; siGFP 5′-GCAAGCUGACCCUGAAG UU-3′.

siRNA transfections of U2OS (20 nM final concentration) were performed with the aid of Lipofectamine RNAiMAX (Invitrogen) according to the manufacturer's instructions. TIG3 BRAF-ER cells were transfected with siRNA (50 nM final concentration) using PEI or plasmid using FuGENE HD (Roche). For the pcDNA3.1-hPRMT6 plasmid, the open reading frame (ORF) sequence of human PRMT6 was generated by BamHI/EcoRI restriction of pGEX-2T-hPRMT6 (6) and cloned into pcDNA3.1 (Invitrogen). The corresponding short hairpin RNA (shRNA) sequences of siPRMT6_1, siPRMT6_2, siPRMT6_3 and siLuci were cloned into pRetro-SUPER Puromycin vector. These plasmids were transfected into the retrovirus producer cell line Phoenix using the calcium phosphate method. ShRNA expression in TIG3-T cells was achieved by repeated infections for 2 days with the virus expressing shRNA constructs. Infected cells were selected with puromycin (1 μg/ml) for 3 days.

Western blot analysis

Cells were washed in cold PBS and subsequently lysed in IPH buffer (50 mM Tris/HCl, pH 8.0, 150 mM NaCl, 5 mM EDTA, 0.5% NP40) for 30 min at 4°C. Debris was removed by centrifugation and protein determination of the clear lysates was performed according to Bradford. Protein extracts (20–30 μg) were analyzed by SDS–PAGE and western blot with the indicated antibodies.

Reverse transcription-quantitative PCR and chromatin immunoprecipitation-quantitative PCR

Total RNA was isolated using the RNA-Mini-Kit (Seqlab) or the RNeasy Micro Kit (Qiagen, for the small cell numbers of the colony formation assay) according to the protocol. Amounts of 10 ng–1 μg RNA were applied to reverse transcription (RT) by incubation with oligo$(dT)_{17}$ primer and 100 U M-MLV RT (Invitrogen), as recommended by the manufacturer. ChIP experiments were performed as described in (6). Complementary DNA and eluted chromatin were subjected to quantitative PCR (qPCR) analysis in triplicates with gene-specific primers. qPCR was performed using Absolute QPCR SYBR Green Mix (Thermo Scientific) and the Mx3000P real-time detection system (Agilent). For RT-qPCR, S14 or Ubiquitin gene transcription was used for normalization. ChIP-qPCR results were expressed as percent input and additionally calculated as fold IgG. Reproducible and representative data sets are shown.

For RT-qPCR, the following primers were used: S14_forward: 5′-GGCAGACCGAGATGAATCCTCA-3′ and S14_reverse 5′-CAGGTCCAGGGGTCTTGGTC C-3′; Ubiquitin_forward: 5′-CACTTGGTCCTGCGCT TGA-3′ and Ubiquitin_reverse: 5′-CAATTGGGAATGC AACAACTTTAT-3′; PRMT6_forward: 5′-AGACACG GACGTTTCAGGAG-3′ and PRMT6_reverse: 5′-CCA CTTTGTAGCGCAGCAG-3′; p21_forward: 5′-GGCAG ACCAGCATGACAGATTTC-3′ and p21_reverse: 5′-CG GATTAGGGCTTCCTCTTGG-3′; p27_forward: 5′-CCCTAGAGGGCAAGTACGAGT-3′ and p27_reverse: 5′-AGTAGAACTCGGGCAAGCTG-3′; p57_forward: 5′-CACGATGGAGCGTCTTGTC-3′ and p57_reverse: 5′-GCTCAGCTCCTCGTGGTC-3′; p16_forward: 5′-CC CCTTGCCTGGAAAGATAC-3′ and p16_reverse: 5′-A GCCCCTCCTCTTTCTTCCT-3′; p15_forward: 5′-GCG GGGACTAGTGGAGAAG-3′ and p15_reverse: 5′-CTG CCCATCATCATGACCT-3′; p14_forward: 5′-CTACTG AGGAGCCAGCGTCT-3′ and p14_reverse: 5′-CTGCCC ATCATCATGACCT-3′; cyclin A2_forward: 5′-ATGAG ACCCTGCATTTGGCTG-3′ and cyclin A2_reverse: 5′-T TGAGGTAGGTCTGGTGAAGG-3′; cyclin D1_ forward: 5′-GACCTCCTCCTCGCACTTC-3′ and cyclin D1_reverse: 5′-CCCTCGGTGTCCTACTTCAA-3′.

For ChIP-qPCR, the following primers were used: p21(−6.8 kb)_forward: 5′-GGAGGGCAAAGTACAGT GGA-3′ and p21(−6.8 kb)_reverse: 5′-CACATGTGACT TGGGGTGAG-3′; p21(−1 kb)_forward: 5′-TACGGGC TATGTGGGGAGTA-3′ and p21(−1 kb)_reverse: 5′-AA GGGGAGGATTTGACGAGT-3′; p21(TSS)_forward: 5′-CCGAAGTCAGTTCCTTGTGG-3′ and p21(TSS)_ reverse: 5′-CGCTCTCTCACCTCCTCTGA-3′; p21 (+0.5 kb) _forward: 5′-GTGGGGATGAAGTCCGTG TC-3′ and p21(+0.5 kb)_reverse: 5′-ACTTACTCCACTC CGCTTTC-3′; p21(+8.6 kb)_forward: 5′-CTGTAAACCT CTCGAGGGCA-3′ and p21(+8.6 kb)_reverse: 5′-GCAC CTGCTGTATATTCAGC-3′; p16(−1.8 kb)_forward: 5′-CTTTTACCTCCTTGCGCTTG-3′ and p16(−1.8 kb) _reverse: 5′-TGGGAGACAAGAGCGAAACT-3′; p16 (−0.5 kb)_forward: 5′-AGGGGAAGGAGAGAGCAG TC-3′ and p16(−0.5 kb)_reverse: 5′-CTACCCCCTCAAC CCTTGAT-3′; p16(TSS)_forward: 5′-CCCCTTGCCTG GAAAGATAC-3′ and p16(TSS)_reverse: 5′-AGCCCCT CCTCTTTCTTCCT-3′; p16(+0.5 kb)_forward: 5′-TCAG GTAGCGCTTCGATTCT-3′ and p16(+0.5 kb)_reverse: 5′-GGCTCCTCATTCCTCTTCCT-3′; p16(+1.0 kb)_ forward: 5′-CCCTTCACTTTGGGAGATCA-3′ and p16(+1.0 kb)_reverse: 5′-CCCCCGGCTACTTTTTGT AT-3′.

Colony formation assay

For colony formation assay, U2OS cells were transfected for 48 h and then 400 cells were plated in triplicates on 6-well plates. After incubation for 10 days, colonies were stained with crystal violet [0.1% (w/v) in 20% ethanol], photographed and counted.

Growth curve analysis (population doublings)

For growth curve analysis, TIG3-T cells were infected, selected and seeded in triplicates in 6-well plates. Subsequently, the cells were passaged according to a 3T3-like protocol. Every third day, the cells were trypsinized, counted and seeded again at a density of 1.5×10^5 cells/well. The cumulative increase in cell number (population doublings) was calculated.

Fluorescence-activated cell sorting assay

For quantification of the cell cycle distribution, TIG3-T cells were harvested, washed in ice-cold PBS and fixed in 80% ethanol at −20°C. After complete permeabilization, cells were washed again and DNA was stained with 54 μM propidium iodide (PI) in the presence of 38 mM sodium citrate and 250 μg/ml RNase A for 30 min at 37°C. Samples were then analyzed in a Becton Dickinson FACS Calibur and reproducible and representative data sets are shown.

Senescence-associated β-galactosidase staining

For detection of senescence, TIG3-T cells were infected, selected for 3 and 7 days later stained for senescence-associated β-galactosidase (SA-β-Gal). OIS was induced in TIG3 BRAF-ER cells upon 4-OHT treatment (200 nM) and subsequently staining for SA-β-Gal was performed at the indicated time points. As previously described (17), the enzymatic activity of SA-β-Gal was detected by using the chromogenic substrat X-Gal, which is converted at pH 6.0 to blue intracellular precipitates. The blue staining was either photographed for qualitative analysis or quantified by counting 3×300 cells and calculating the percentage of SA-β-Gal-positive cells.

RESULTS

PRMT6 facilitates the clonogenic growth of U2OS cells

As PRMT6 overexpression has been observed in several tumor entities (13), we asked whether the enzyme is required for survival and proliferation of transformed cells. To address this question, we employed the human osteosarcoma cell line U2OS in a clonogenic assay or so-called colony formation assay, which measures the

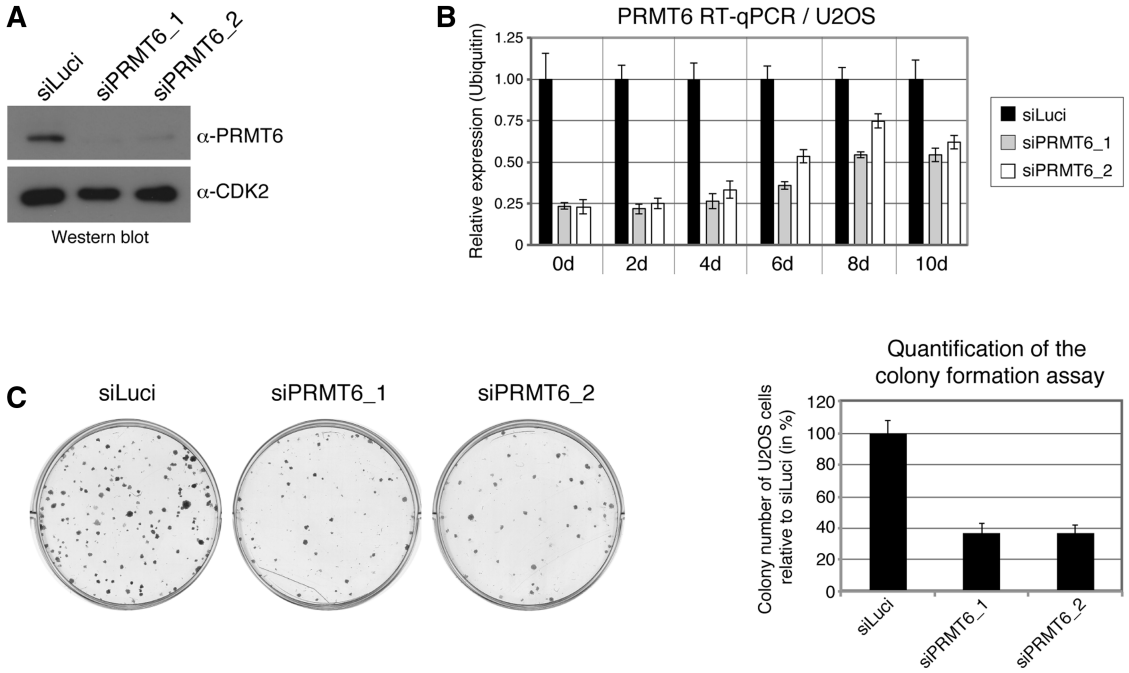

Figure 1. Depletion of PRMT6 inhibits the colony formation in U2OS cells. (**A**) U2OS cells were transfected with siLuci or two alternative siRNAs directed against PRMT6 (siPRMT6_1 or siPRMT6_2) and harvested 72 h post transfection. Total protein (30 μg) of each sample was analyzed by western blot with the indicated antibodies. (**B** and **C**) U2OS cells were transfected with siRNAs as in (A). Forty-eight hours post transfection cells were replated for (B) preparation of total RNA and in triplicates for (C) colony formation assay. RNA was prepared at the indicated time points (0, 2, 4, 6, 8 and 10 days) and analyzed by RT–qPCR for the transcript levels of PRMT6 normalized to Ubiquitin (siLuci in black bars, siPRMT6_1 in gray bars, siPRMT6_2 in white bars). The colony formation assay was evaluated after 10 days. Representative dishes of crystal violet-stained colonies were photographed (left panel). The number of colonies was counted (right panel) and the quantification is presented as colony number in percentage of the siPRMT6 conditions relative to siLuci condition (the latter equated 100%). The result shown is the average of the triplicate countings (±SD).

ability of single cells plated in very low density to survive and to grow into colonies due to their unlimited division potential. For these studies, we established transfection of two alternative siRNAs directed against PRMT6 (siPRMT6_1 and siPRMT6_2) and one control siRNA (siLuci) in U2OS cells and achieved efficient depletion of PRMT6 protein with both PRMT6-specific siRNAs (Figure 1A). PRMT6-depleted and control U2OS cells were plated in low density and subsequently cultured for 10 days. After 10 days, colonies were stained with crystal violet and counted. In parallel, the knockdown efficiency of PRMT6 was determined on RNA level over this time period revealing that the transcript levels of PRMT6 were reduced to 25% by the two specific siRNAs compared to the control siRNA at the day of plating (0 day). The efficiency of depletion declined during 10 days of culturing, but PRMT6 mRNA levels were still reduced to 60% at final day (10 days) (Figure 1B). When counting the colonies, we found that depletion of PRMT6 with both siRNAs causes a reduction in the colony numbers of at least 60% compared to control siRNA transfected cells (Figure 1C). This suggests that PRMT6 depletion limits the proliferation capability of the cells and might lead to cell cycle arrest.

The CDK inhibitor p21 is a direct transcriptional target of PRMT6 in U2OS cells

To answer whether important cell cycle regulators, such as CDKs, CDK inhibitors and cyclins are involved in these PRMT6-dependent proliferation effects, we determined the protein levels of the CDK2, of CDK inhibitors p21 ($p21^{CIP1/WAF1}$, CDKN1A) and p27 ($p27^{KIP1}$, CDKN1B) of the CIP/KIP family and of cyclin A2 (CCNA2) in PRMT6-depleted U2OS cells. The INK4A/B locus, which encodes the CDK inhibitors of the INK4 family, was not studied, as it is inactivated by deletion and DNA methylation in U2OS cells (18,19). We employed in these siRNA experiments additional transfection controls and three additional alternative siRNA sequences targeting PRMT6. All five independent siPRMT6 sequences produced an efficient knockdown of PRMT6 on protein as well as RNA level compared to untransfected or control transfected cells (Figure 2A and B). The PRMT6 depletion was accompanied by an increase in p21 protein levels, whereas expression of CDK2 was not affected and expressions of p27 as well as cyclin A2 were not uniformly affected by the knockdown with the different siPRMT6 compared to the controls (Figure 2A). These data indicate that PRMT6 selectively influences the expression of the p21 protein.

Given that PRMT6 has a well-established function as a transcriptional coregulator (6,9–11), we next investigated by RT–qPCR analysis whether PRMT6 might affect p21 and other cell cycle regulators at the transcriptional level. In agreement with the increased p21 protein levels, depletion of PRMT6 with the different siPRMT6 led to a 2- to 5-fold increase in p21 mRNA levels in comparison to the controls (Figure 2C). Transcript levels of p27 and the third

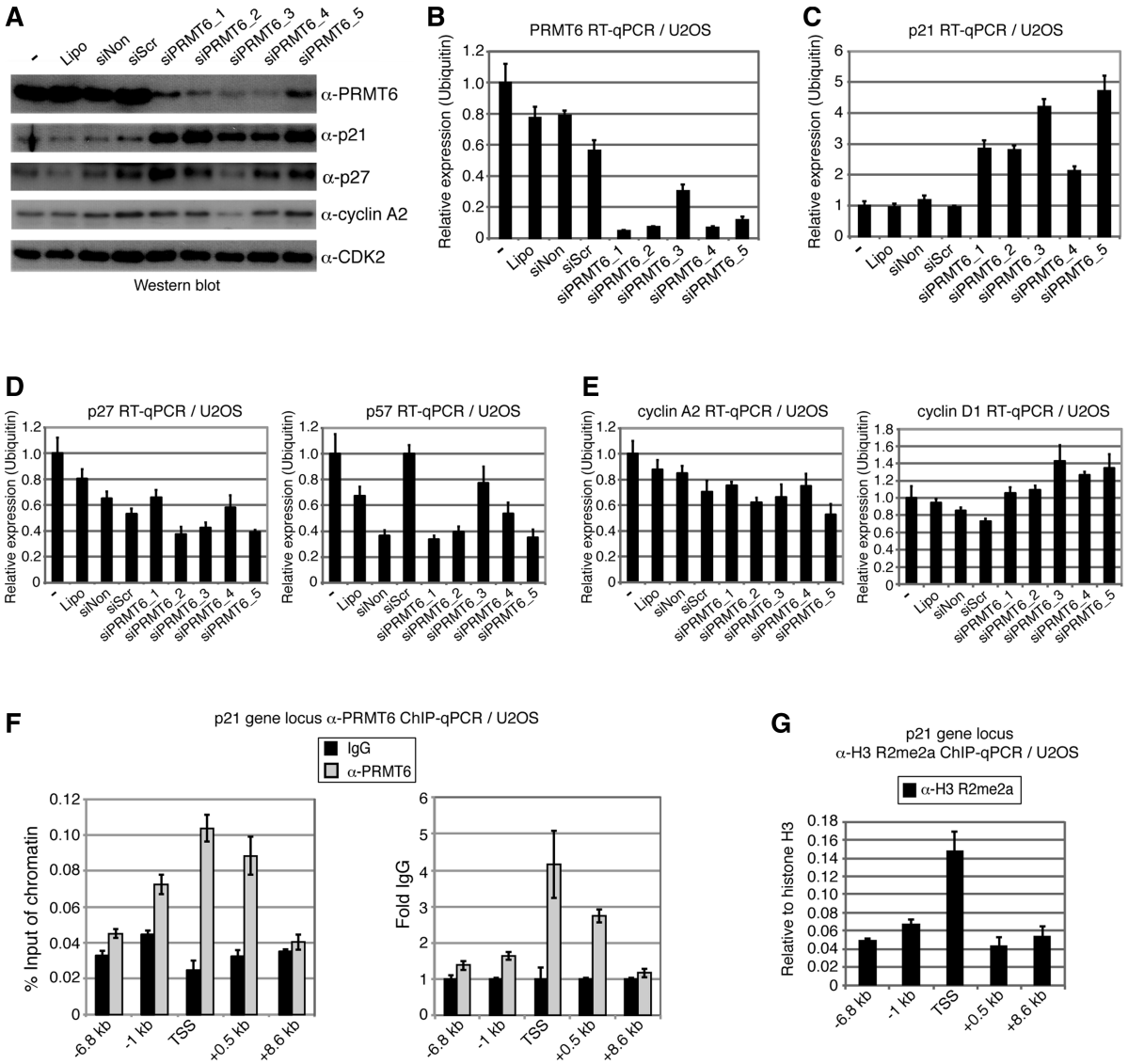

Figure 2. PRMT6 regulates p21 gene expression in U2OS cells and is recruited to the p21 gene locus accompanied by enhanced H3 R2me2a level. (**A**) U2OS cells were transfected with siNon-targeting (siNon), siScramble (siScr) or five alternative siRNAs against PRMT6 (siPRMT6_1, _2, _3, _4, _5). Additional controls were untransfected cells (−) and Lipofectamine RNAiMAX (Lipo)-treated cells. Seventy-two hours post transfection cells were harvested and 30 µg total protein of each sample were analyzed by western blot with the indicated antibodies. (**B–E**) U2OS cells were treated with siRNAs or control conditions as in (A) for 72 h. Subsequently, cells were harvested and total RNA was prepared and analyzed by RT–qPCR for transcript levels of (B) PRMT6, (C) p21, (D) p27 and p57, (E) cyclin A2 and D1, respectively, normalized to Ubiquitin. (**F** and **G**) U2OS cells were harvested after 72 h and subjected to ChIP analysis using antibodies against (F) PRMT6 (gray bars) and corresponding control antibody (black bars, IgG rabbit) or (G) H3 R2me2a and corresponding control antibody (H3). Immunoprecipitated DNA was analyzed in triplicates by qPCR with primers spanning the indicated regions of the p21 gene locus. In (F), mean values were expressed as percent input of chromatin or as fold IgG, which was equated 1. In (G), mean values were expressed as relative enrichment compared to histone H3.

member of the CIP/KIP family p57 ($p57^{KIP2}$, CDKN1C) (Figure 2D) and of cyclin A2 and D1 (Figure 2E) were not uniformly regulated by the different siPRMT6. They were either reduced (p27, p57, cyclin A2) or slightly enhanced (cyclin D1) or not altered in comparison to the control conditions (Figure 2D and E). Taken together, these results show that PRMT6 selectively represses p21 gene transcription, but does not affect other members of the CIP/KIP family or cyclin A2 and D1.

To examine whether p21 is a direct target gene of this PRMT6-mediated repression, we performed chromatin immunoprecipitation (ChIP) analysis in U2OS cells and found that PRMT6 associates strongly (3- to 4-fold above the IgG control) with the transcriptional start site (TSS) and the transcribed region (+0.5 kb) of the p21 gene, but not with the upstream (−1 and −6.8 kb) or downstream (+8.6 kb) regions of the gene locus (Figure 2F). To elucidate whether PRMT6 recruitment coincides with the corresponding histone methyltransferase activity, the distribution of H3 R2me2a at the p21 gene locus was also determined in ChIP analysis. We found that the H3 R2me2a mark was 3-fold enriched specifically at the TSS of the p21 gene in comparison to the other regions investigated (Figure 2G). The observation that both

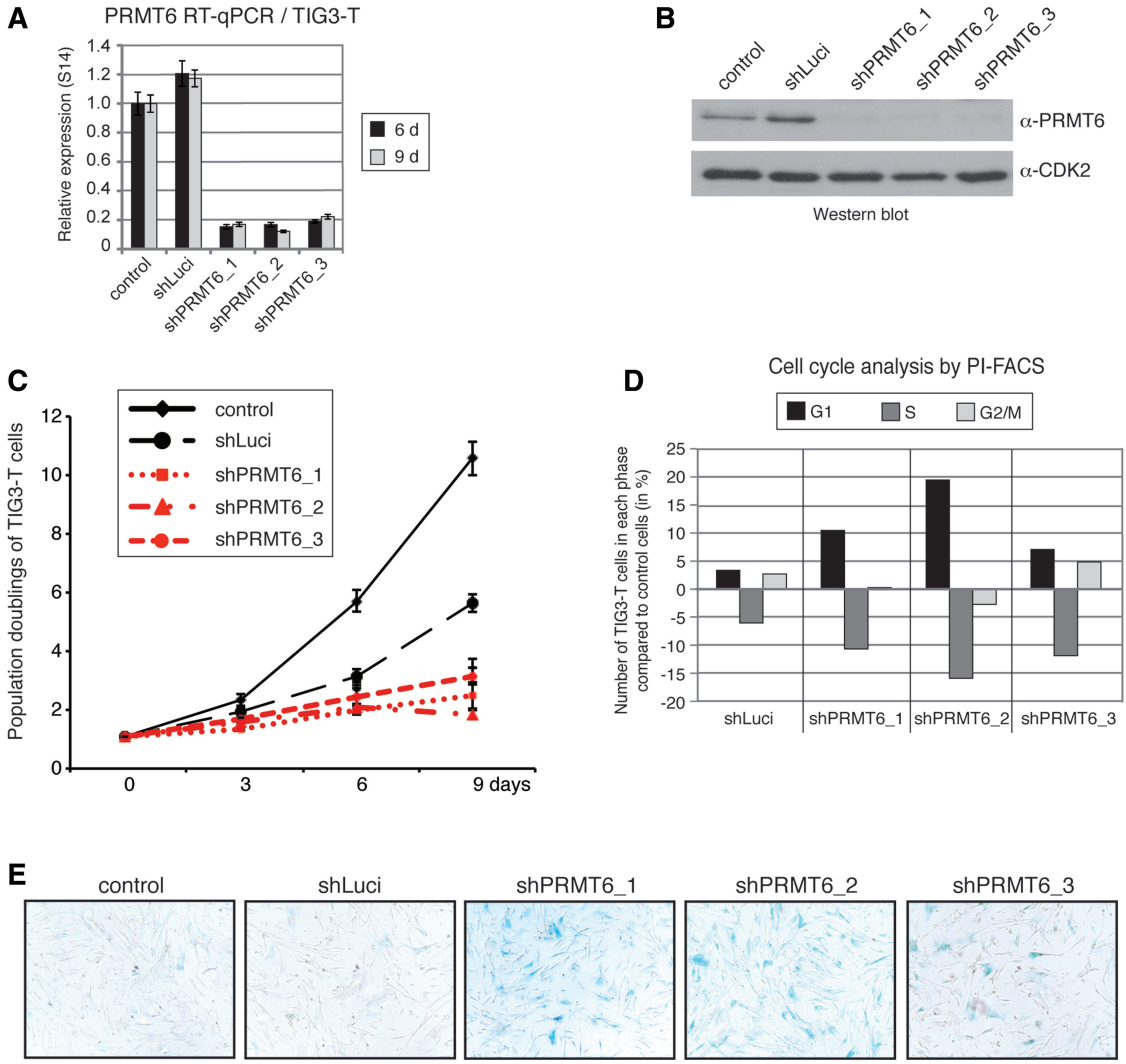

Figure 3. Depletion of PRMT6 results in a reduced cell proliferation rate, an accumulation of cells in G1-phase and enhanced senescence in TIG3-T cells. (**A** and **B**) TIG3-T cells were infected with retroviral vectors coding for shLuci or three alternative shRNA against PRMT6 (shPRMT6_1, _2, _3). Infections with empty vector served as an additional control. Forty-eight hours post infection cells were selected with puromycin (1 μg/ml) for 72 h. After 6 and 9 days, respectively, of shRNA-mediated depletion (Day 0 corresponds to 3 days after start of selection), cells were harvested and analyzed for (A) RNA and (B) protein. Total RNA from cells with 6 (black bars) or 9 days (gray bars) of shRNA expression was prepared and analyzed by RT–qPCR for PRMT6 transcript levels normalized to S14. Total protein (20 μg) of each sample (9 days only) were analyzed by western blot with the indicated antibodies. (**C–E**) TIG3-T cells were infected with shRNA constructs and selected with puromycin as in (A and B). (C) Representative growth curves of TIG3-T cells are shown in which cells were seeded for 3T3 assay up to 9 days. Day 0 is the time point of plating for the 3T3 assay and corresponds to 3 days after start of selection. (D) After 7 days of shRNA-mediated depletion (Day 0 corresponds to 3 days after start of selection), cells were fixed, stained with PI and analyzed by flow cytometry for G1 (black bars), S (dark gray bar) and G2/M-phase (bright gray bars). Data show changes in each phase of cell cycle (in percent) relative to control cells (empty vector) and are representative results of several independent experiments. (E) After 7 days of shRNA-mediated depletion (Day 0 corresponds to 3 days after start of selection), cells were stained for SA-β-Gal activity. SA-β-Gal staining was photographed using a bright field microscope. Data show a representative result of several independent experiments.

PRMT6 and H3 R2me2a peak at the TSS of the p21 gene indicates that p21 is a direct target gene of the H3 R2me2a-associated repressive activity of PRMT6 and might be responsible for the pro-proliferative function of PRMT6 in transformed cells.

PRMT6 facilitates cell proliferation and blocks senescence of TIG3-T cells

Next, we asked whether PRMT6 similarly controls proliferation of non-transformed cells. For these studies, we chose telomerase-immortalized TIG3-T human diploid fibroblasts and infected these cells with retroviral vectors encoding shRNAs (identical to the corresponding siRNA sequences), targeting PRMT6 or luciferase (shLuci). The three independent shRNAs directed against PRMT6 achieved an efficient depletion within a time period of up to 9 days on RNA and protein level (Figure 3A and B). When we measured population doublings for 9 days in control (empty vector), shLuci- and shPRMT6-infected cells, we found that depletion of PRMT6 leads to a considerable slowdown of cell proliferation compared to

control and shLuci infection (Figure 3C). To clarify whether this growth-inhibitory effect is caused by defective cell cycle progression, we stained the DNA of infected TIG3-T cells with PI and analyzed their cell cycle distribution by fluorescence-activated cell sorting (FACS). Similar to the population doubling analysis, the FACS profile revealed that even infection with shLuci slightly inhibits cell cycle progression, as indicated by the increased cell number in G1-phase (by 3.5%) and reduced cell number in S-phase (by 6%) compared to control-infected cells (Figure 3D). However, the effects of PRMT6 depletion were clearly more dramatic, as all three shPRMT6 constructs resulted in a 7.5–20% increased cell number in G1-phase and in a 10–15% reduced cell number in S-phase compared to the control-infected cells (Figure 3D). These findings reveal that depletion of PRMT6 gives rise to a cell cycle arrest in G1-phase. Hence, PRMT6 facilitates proliferation also in non-transformed immortalized cells.

Knowing that a continuous arrest in G1-phase is a typical feature of senescence and that some PRMT6-depleted TIG-3 cells showed a flat, enlarged senescence-like morphology (data not shown), we examined whether PRMT6 knockdown is accompanied by induction of senescence. We measured levels of SA-β-Gal, a biomarker for senescent cells. In this way, we found that the number and strength of SA-β-Gal-positive cells was significantly enhanced in the PRMT6-depleted conditions compared to the control and shLuci infections (Figure 3E). These results show that in agreement with its pro-proliferative function, PRMT6 is also crucial for suppressing the onset of senescence.

PRMT6 represses the expression of p21 as well as p16 in TIG3-T cells

To answer the question whether PRMT6 affects similar target genes that might account for the proliferation effects of PRMT6 in non-transformed cells as it does in tumor cells, we analyzed the expression of the candidate target gene p21 in shPRMT6-depleted TIG3-T cells. Additionally, as the INK4A/B locus is not mutated and is therefore active in TIG3-T cells, the cell system allowed us to study the impact of PRMT6 on the expression of this second class of CDK inhibitors. Depletion of PRMT6 with the three independent shRNAs led to upregulation of both p21 and p16 ($p16^{INK4A}$, CDKN2A) on protein as well as RNA levels (Figure 4A and B). In contrast, the two other genes of the INK4A/B tumor suppressor locus, the p14 ($p14^{ARF}$) gene, which represent an alternative reading frame, and the adjacent CDK inhibitor gene p15 ($p15^{INK4B}$, CDKN2B), were not influenced in their mRNA levels upon PRMT6 knockdown (Figure 4C). These data show that PRMT6 represses a selective set of cell cycle inhibitors and tumor suppressors on the transcriptional level also in non-transformed cells.

To elucidate whether p21 and p16 are directly regulated by PRMT6 in TIG3-T cells, we performed ChIP analysis and detected that PRMT6 is predominantly bound to the TSS and to a lower extent also to the transcribed region (+0.5 kb) of p21 (Figure 4D), similar to its occupancy at this gene locus in U2OS cells. Furthermore, PRMT6 and H3 R2me2a peaks coincided at the TSS of the p21 gene (Figure 4E). For the p16 gene, we found that the −0.5 kb region as well as the TSS were predominantly occupied by PRMT6 (3-fold above the IgG control) and to a lower extent also the transcribed regions (+0.5 and +1.0 kb) in comparison to the control region (−1.8 kb) (Figure 4F). In contrast, H3 R2me2a was not detectable at the p16 gene above background level of the control region, suggesting that the appearance of PRMT6 and H3 R2me2a does not correlate here (Figure 4G). These findings identify p21 and p16 as important downstream targets of PRMT6 that explain its function as positive regulator of proliferation and as negative regulator of senescence. However, these two target genes might be differentially regulated by PRMT6 as the histone methyltransferase activity correlates with repression of p21, whereas repression of p16 is not accompanied by H3 R2me2a at the gene locus.

PRMT6 is downregulated and p21 is activated during OIS

Finally, we investigated the potential relationship between PRMT6 and p21 in a cell model of OIS, the TIG3 BRAF-ER cells. These cells express an oncogenic (constitutively active) form of BRAF, a serine/threonin-specific kinase of the MAPK pathway, fused to the ligand-binding domain of the ER. The activity of BRAF within this fusion protein is induced upon 4-OHT addition, rapidly leading to cell cycle arrest and the occurrence of senescence (15,16), which we detected within a time period of up to 6 days of 4-OHT treatment as measured by SA-β-Gal staining (Figure 5A). In this model of OIS, we found for p21 and p16, which are important and well-known inducers of senescence, that their transcript levels increase upon the onset of senescence and reach after 8 days of 4-OHT stimulation a 4.5-fold increase for p21 and a 3.5-fold increase for p16 compared to untreated TIG3 BRAF-ER cells (Figure 5B). In contrast, p27 and p14 were either reduced or only moderately enhanced in their mRNA levels during senescence induction (Figure 5C).

Knowing from our present data that p21 and p16 are both direct target genes of PRMT6, whereas p27 and p14 are not, we next asked whether expression of PRMT6 is affected after induction of OIS. We found that PRMT6 is downregulated on RNA as well as protein levels concomitantly with the establishment of the senescent cell phenotype (Figure 5D and E). After 8 days of 4-OHT stimulation, the transcript level of PRMT6 was reduced to 40% (Figure 5D). This indicates that PRMT6 and its target genes p21 and p16 are inversely regulated during OIS and that OIS-associated downregulation of PRMT6 likely allows transcriptional induction of p21 and p16.

Given that p21 shows a strong OIS-associated transcriptional upregulation (up to 4.5-fold in comparison to the untreated condition), we wished to elucidate the relevance of p21 for OIS in this cell model. To address this issue, we reduced p21 levels in TIG3 BRAF-ER cells using siRNA transfection and subsequently induced senescence with 4-OHT. Depletion of p21, which was confirmed by

RT–qPCR in comparison to the control siGFP transfection (Figure 5F), impaired the extent of OIS measured by SA-β-Gal staining (Figure 5G). These data demonstrate that p21 is essential for this senescent phenotype.

Finally, we wished to clarify whether PRMT6 is indeed important for the induction of OIS. We transfected TIG3 BRAF-ER cells with empty vector (control) or an PRMT6 overexpression construct and subsequently induced senescence by addition of 4-OHT. Overexpression of PRMT6 was confirmed by RT–qPCR (Figure 5H). We found that OIS was detectable in empty vector-transfected cells after 2 days and was further enhanced after 4 days of 4-OHT

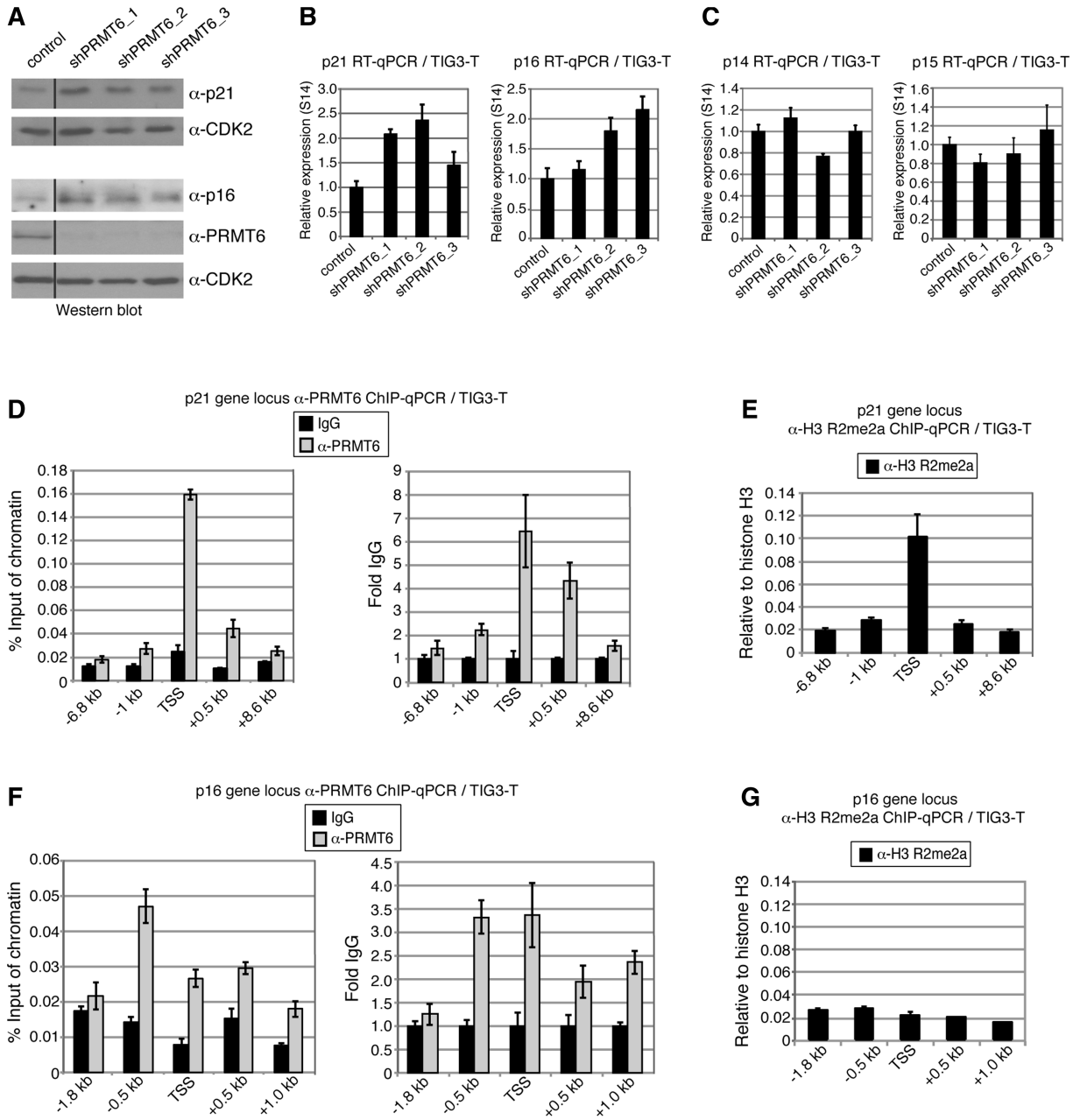

Figure 4. The cell cycle regulators p21 and p16 are direct transcriptional targets of PRMT6 in TIG3-T cells. (**A**) TIG3-T cells were infected with three alternative shRNA vectors against PRMT6 (shPRMT6_1, _2, _3). The empty vector served as control. Forty-eight hours post infection cells were selected with puromycin (1 μg/ml) for 72 h. After 6 days of shRNA-mediated depletion (Day 0 corresponds to 3 days after start of selection), cells were harvested and 20 μg total protein of each sample were analyzed by western blot with the indicated antibodies. The black line indicates that the scan was cut at this point, but all stainings shown are from the same blot and exposure time. (**B** and **C**) TIG3-T cells were treated as in (A). Total RNA was prepared and analyzed by RT–qPCR for (B) p21 and p16 and (C) p14 and p15 transcript levels normalized to S14. (**D–G**) TIG3-T cells were harvested after 72 h and subjected to ChIP analysis using antibodies against (D and F) PRMT6 (gray bars) and corresponding control antibody (black bars, IgG rabbit) or (E and G) H3 R2me2a and corresponding control antibody (H3). Immunoprecipitated DNA was analyzed in triplicates by qPCR with primers spanning the indicated regions of the (D and E) p21 and (F and G) p16 gene locus. In (D and F), mean values were expressed as percent input of chromatin or as fold IgG, which was equated 1. In (E and G), mean values were expressed as relative enrichment compared to histone H3.

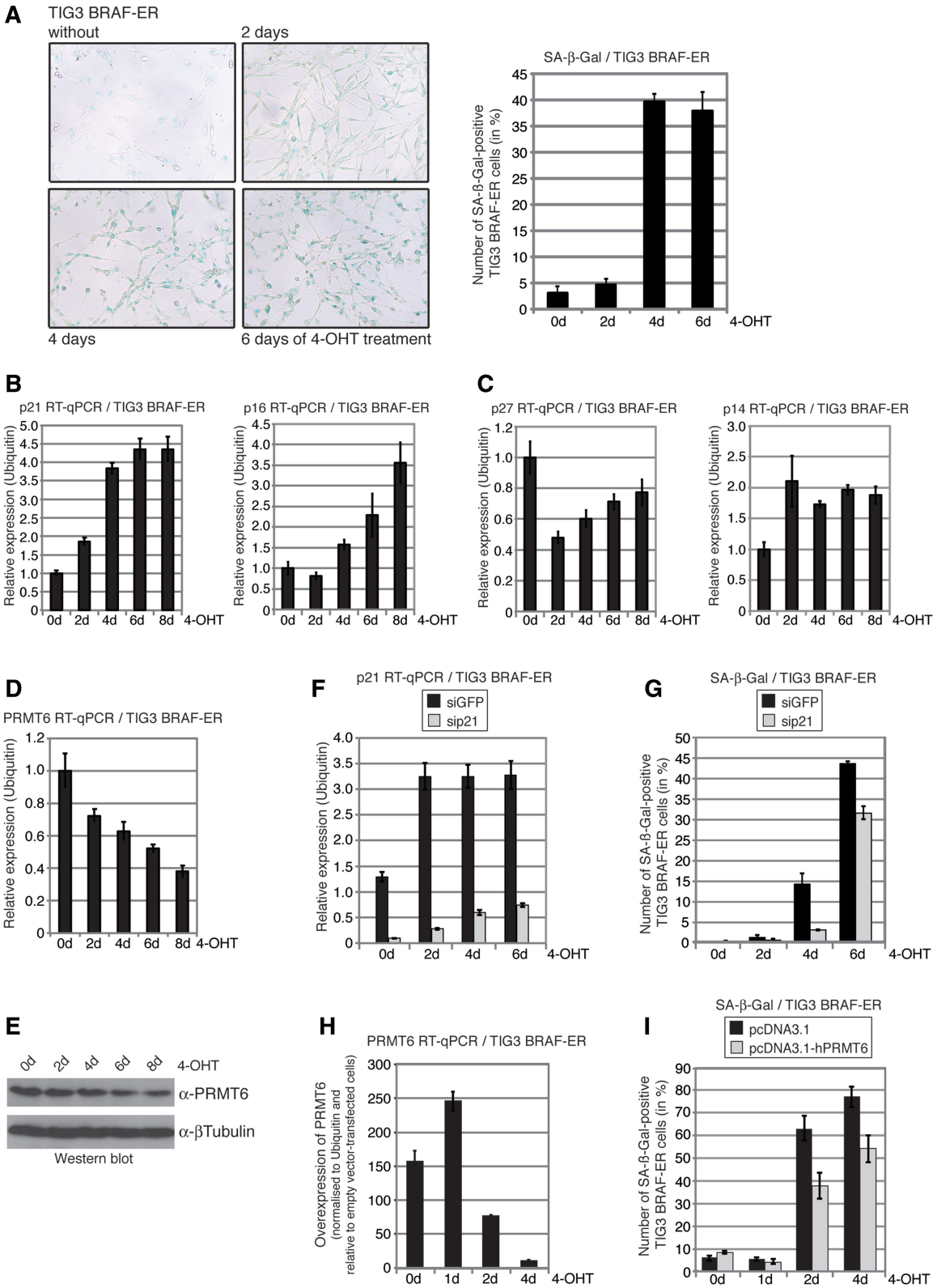

Figure 5. Effects of OIS on PRMT6 and p21 expression in TIG3 BRAF-ER cells and the relevance of PRMT6 and p21 in this model of OIS. (**A**) TIG3 BRAF-ER cells were treated with 4-OHT (200 nM) and stained for SA-β-Gal activity at the indicated time points. SA-β-Gal staining was photographed using a bright field microscope (left panel). The number of SA-β-Gal-positive TIG3 BRAF-ER cells was quantified (right panel). The presented result in percentage is the average from triplicate countings (each with 300 cells) ± SD. Data show a representative result of several independent experiments. (**B–E**) TIG3 BRAF-ER cells were treated with 4-OHT as in (A). (B–D) Total RNA was prepared and analyzed by RT–qPCR for the transcript levels of (B) p21 and p16 and (C) p27 and p14 and (D) PRMT6 at the indicated time points normalized to Ubiquitin. (E) Cells were harvested at the indicated time points and 20 μg total protein of each sample were analyzed by western blot with the indicated antibodies. (**F** and **G**) TIG3 BRAF-ER cells were transfected with siGFP or siRNAs (pool of three sequences) directed against the

(continued)

treatment. Overexpression of PRMT6 reduced the levels of OIS at Days 2 and 4 when compared to the control cells (Figure 5I). Taken together, these findings identify PRMT6 as an important negative regulator of senescence. Our results suggest that the pro-proliferative and anti-senescence function of PRMT6 might be explained by its repressive function on p21 as well as p16 gene expression.

DISCUSSION

In the present work, we identify PRMT6 as a positive regulator of proliferation and a negative regulator of senescence. The CDK inhibitor genes p21 of the CIP/KIP family and p16 of the INK4 family were determined as the two important downstream targets, which are transcriptionally repressed by PRMT6 and responsible for mediating these cellular functions of PRMT6. The p21 protein is known to bind several CDKs, in particular CDK1 and CDK2, and their corresponding cyclins leading to inhibition of the kinase activity and interfering with activating phosphorylations of the CDKs. In contrast, p16 specifically interacts with CDK4 and CDK6 augmenting their ability to bind cyclin D and to phosphorylate and inhibit the retinoblastoma protein (20). Both CDK inhibitors block cell cycle progression in response to a variety of stimuli; for example, mitogens, DNA-damage and oxidative stress, and promote cellular senescence. p21 achieves growth arrest in G1- as well as G2-phase of the cell cycle, whereas p16 selectively inhibits the progression through early G1 phase. The fact that PRMT6 represses transcription of both CDK inhibitor genes agrees with our observation that PRMT6-depleted cells succumb to G1 arrest, slowdown their proliferation rate and undergo senescence.

Consistently with its target genes p21 and p16, which are tumor suppressors and frequently silenced in human cancer thereby allowing deregulation of CDK activity and enforcement of cell cycle progression (21), PRMT6 has been found to be overexpressed in certain malignancies. Our findings in U2OS cells conform to reports on the positive role of PRMT6 on tumor cell survival, for example of bladder and lung cancer cells and of estrogen-stimulated breast cancer cells (12,13). Furthermore, maintenance of asymmetric dimethylation of arginines within substrate proteins correlates with highly proliferative cells (22). Accordingly, expression levels of several PRMT family members, including PRMT6, were found to be elevated in young cells and to decline in replicative and stress-induced senescent cells (22). As we found that PRMT6 transcript levels decline during OIS, the question arises by which mechanism and transcription factors gene expression of PRMT6 itself is regulated during senescence. Until now, only a few studies have dealt with the issue of how PRMT genes in general are transcriptionally controlled. A recent report identified a c-Myb binding site in the first intron of the PRMT1 gene and revealed that c-Myc is responsible for activation of PRMT1 transcription during *Xenopus* metamorphosis (23).

Interestingly, PRMT6 does not control the expression of all members of the two CDK inhibitor families. We found that p27 and p57 as well as p15 were not specifically affected in their transcript as well as protein levels by PRMT6, rather the enzyme seems selectively to affect a subset of important cell cycle regulators. Consistently, also cyclins, of which we exemplarly analyzed cyclin D1 and A2, were not altered in their expression by PRMT6. Even for the regulation of p21 and p16, we showed that they are differentially regulated by PRMT6. In case of the p21 gene locus, the PRMT6 recruitment pattern overlapped with the presence of the H3 R2me2a mark and both peak at the TSS. This indicates that the histone-modifying activity of PRMT6 might be required for its repressive activity at the p21 gene potentially by counteracting H3 K4me3 or its recognition by effector proteins (6,9,10). In contrast, although PRMT6 bound to the TSS and neighboring regions of the p16 gene, the corresponding histone mark was not enriched at these sites. Therefore, it seems possible that repression of p16 does not need the histone methyltransferase activity of PRMT6. It is conceivable that PRMT6 similar to other PRMTs modifies transcriptional coregulators, like histone acetyltransferases, or also transcription factors, like SMADs, ER or Runt-related transcription factor 1 (RUNX1), and in this way fulfills its repressive function (3). Given that PRMT6 methylates the viral transactivator Tat, such a scenario seems possibly (8). Alternatively, PRMT6 might function as an adaptor protein and responsible for the recruitment of other effectors, which then accomplish gene silencing. So far the general importance of the catalytic activity of PRMTs in gene regulation was demonstrated only for PRMT4 (24), which leaves the possibility of a methyltransferase-independent repression by PRMT6 open.

Given that PRMT6 is not able to directly bind target genes, the question arises how PRMT6 is recruited to the

Figure 5. Continued
p21 transcript. Forty-eight hours post transfection cells were treated with 4-OHT (200 nM) for the indicated time course (Day 0 corresponds to 2 days after start of siRNA-mediated depletion). Total RNA of the siGFP (black bars) and sip21 conditions (gray bars) was prepared and analyzed by RT–qPCR for the transcript levels of (F) p21 normalized to Ubiquitin. SA-β-Gal-positive cells (G) were counted at the indicated time points either for siGFP- (black bars) or sip21-depleted cells (gray bars). The presented result in percentage is the average from triplicate countings (each with 300 cells) ± SD. Data show a representative result of several independent experiments. (**H** and **I**) TIG3 BRAF-ER cells were transfected with empty vector (pcDNA3.1) or pcDNA3.1-hPRMT6 plasmid. Forty-eight hours post transfection cells were treated with 4-OHT (200 nM) for the indicated time points (Day 0 corresponds to 2 days after start of transfection). Total RNA was prepared and analyzed by RT–qPCR for the transcript levels of (H) PRMT6 normalized to Ubiquitin. Transcript levels of PRMT6 upon overexpression are shown relative to the PRMT6 levels of empty vector-transfected conditions, which were set to 1 for each time point (0, 1, 2 and 4 days). SA-β-Gal-positive cells (I) were counted at the indicated time points either for empty vector (pcDNA3.1)-transfected (black bars) or pcDNA3.1-hPRMT6-transfected cells (gray bars). The presented result in percentage is the average from triplicate countings (each with 300 cells) ± SD. Data show a representative result of several independent experiments.

p21 and p16 gene. Several mechanisms have been reported how the transcription factor Myc, which is frequently overexpressed in tumors and causes deregulated expression of p21, represses transcription of the p21 gene. On the one hand, Myc represses by interacting with the transcription factor Sp1 and blocking the transcriptional activation function of Sp1 at the p21 gene (25). On the other hand, Myc is recruited via the transcription factor Miz1 together with the DNA methyltransferase DNMT3a to the Miz1 binding sites in the p21 gene promoter and alters the chromatin structure into a repressive state (26). Repression of the p16 gene locus is mediated by the Polycomb group proteins that are directly recruited to the gene locus either by the H3 K27me3 mark, long non-coding RNAs or certain transcription factors, such as Zfp277 (27). Whether PRMT6 employs one of these repression mechanisms for its recruitment needs to be clarified in the future.

Taken together, the here identified repressive function of PRMT6 on the expression of the tumor suppressor genes p21 and p16 gives a first explanation why PRMT6 belongs to a cellular program that inhibits senescence and facilitates cell cycle progression and why overexpression of PRMT6 is advantageous to cellular transformation. These findings turn PRMT6 into an attractive target for tumor-preventing research and strategies in the future.

ACKNOWLEDGEMENTS

We are grateful to Kristian Helin for providing the TIG3-T and TIG3 BRAF-ER cells. We thank Inge Sprenger for technical assistance. We thank Alexander Brehm and all members of the U.M.B. laboratory for their suggestions and help.

FUNDING

Deutsche Forschungsgemeinschaft [FOR531, TRR81, TRR17 and Ba 2292/1]; Landes-Offensive zur Entwicklung Wissenschaftlich-ökonomischer Exzellenz 'Tumor and Inflammation'; Bundesministerium für Bildung und Forschung (to U.M.B.). Funding for open access charge: DFG [FOR 531 and TRR81].

Conflict of interest statement. None declared.

REFERENCES

1. Bedford,M.T. and Clarke,S.G. (2009) Protein arginine methylation in mammals: who, what, and why. *Mol. Cell*, **33**, 1–13.
2. Di Lorenzo,A. and Bedford,M.T. (2011) Histone arginine methylation. *FEBS Lett.*, **585**, 2024–2031.
3. Lee,Y.H. and Stallcup,M.R. (2009) Minireview: protein arginine methylation of nonhistone proteins in transcriptional regulation. *Mol. Endocrinol.*, **23**, 425–433.
4. Frankel,A., Yadav,N., Lee,J., Branscombe,T.L., Clarke,S. and Bedford,M.T. (2002) The novel human protein arginine N-methyltransferase PRMT6 is a nuclear enzyme displaying unique substrate specificity. *J. Biol. Chem.*, **277**, 3537–3543.
5. Lakowski,T.M. and Frankel,A. (2008) A kinetic study of human protein arginine N-methyltransferase 6 reveals a distributive mechanism. *J. Biol. Chem.*, **283**, 10015–10025.
6. Hyllus,D., Stein,C., Schnabel,K., Schiltz,E., Imhof,A., Dou,Y., Hsieh,J. and Bauer,U.M. (2007) PRMT6-mediated methylation of R2 in histone H3 antagonizes H3 K4 trimethylation. *Genes Dev.*, **21**, 3369–3380.
7. El-Andaloussi,N., Valovka,T., Toueille,M., Steinacher,R., Focke,F., Gehrig,P., Covic,M., Hassa,P.O., Schar,P., Hubscher,U. *et al.* (2006) Arginine methylation regulates DNA polymerase beta. *Mol. Cell*, **22**, 51–62.
8. Boulanger,M.C., Liang,C., Russell,R.S., Lin,R., Bedford,M.T., Wainberg,M.A. and Richard,S. (2005) Methylation of Tat by PRMT6 regulates human immunodeficiency virus type 1 gene expression. *J. Virol.*, **79**, 124–131.
9. Guccione,E., Bassi,C., Casadio,F., Martinato,F., Cesaroni,M., Schuchlautz,H., Luscher,B. and Amati,B. (2007) Methylation of histone H3R2 by PRMT6 and H3K4 by an MLL complex are mutually exclusive. *Nature*, **449**, 933–937.
10. Iberg,A.N., Espejo,A., Cheng,D., Kim,D., Michaud-Levesque,J., Richard,S. and Bedford,M.T. (2008) Arginine methylation of the histone H3 tail impedes effector binding. *J. Biol. Chem.*, **283**, 3006–3010.
11. Michaud-Levesque,J. and Richard,S. (2009) Thrombospondin-1 is a transcriptional repression target of PRMT6. *J. Biol. Chem.*, **284**, 21338–21346.
12. Harrison,M.J., Tang,Y.H. and Dowhan,D.H. (2010) Protein arginine methyltransferase 6 regulates multiple aspects of gene expression. *Nucleic Acids Res.*, **38**, 2201–2216.
13. Yoshimatsu,M., Toyokawa,G., Hayami,S., Unoki,M., Tsunoda,T., Field,H.I., Kelly,J.D., Neal,D.E., Maehara,Y., Ponder,B.A. *et al.* (2011) Dysregulation of PRMT1 and PRMT6, Type I arginine methyltransferases, is involved in various types of human cancers. *Int. J. Cancer*, **128**, 562–573.
14. Bracken,A.P., Kleine-Kohlbrecher,D., Dietrich,N., Pasini,D., Gargiulo,G., Beekman,C., Theilgaard-Monch,K., Minucci,S., Porse,B.T., Marine,J.C. *et al.* (2007) The Polycomb group proteins bind throughout the INK4A-ARF locus and are disassociated in senescent cells. *Genes Dev.*, **21**, 525–530.
15. Woods,D., Parry,D., Cherwinski,H., Bosch,E., Lees,E. and McMahon,M. (1997) Raf-induced proliferation or cell cycle arrest is determined by the level of Raf activity with arrest mediated by p21Cip1. *Mol. Cell Biol.*, **17**, 5598–5611.
16. Agger,K., Cloos,P.A., Rudkjaer,L., Williams,K., Andersen,G., Christensen,J. and Helin,K. (2009) The H3K27me3 demethylase JMJD3 contributes to the activation of the INK4A-ARF locus in response to oncogene- and stress-induced senescence. *Genes Dev.*, **23**, 1171–1176.
17. Dimri,G.P., Lee,X., Basile,G., Acosta,M., Scott,G., Roskelley,C., Medrano,E.E., Linskens,M., Rubelj,I., Pereira-Smith,O. *et al.* (1995) A biomarker that identifies senescent human cells in culture and in aging skin in vivo. *Proc. Natl Acad. Sci. USA*, **92**, 9363–9367.
18. Miller,C.W., Aslo,A., Campbell,M.J., Kawamata,N., Lampkin,B.C. and Koeffler,H.P. (1996) Alterations of the p15, p16,and p18 genes in osteosarcoma. *Cancer Genet. Cytogenet.*, **86**, 136–142.
19. Park,Y.B., Park,M.J., Kimura,K., Shimizu,K., Lee,S.H. and Yokota,J. (2002) Alterations in the INK4a/ARF locus and their effects on the growth of human osteosarcoma cell lines. *Cancer Genet. Cytogenet.*, **133**, 105–111.
20. Malumbres,M. and Barbacid,M. (2005) Mammalian cyclin-dependent kinases. *Trends Biochem. Sci.*, **30**, 630–641.
21. Malumbres,M. and Barbacid,M. (2009) Cell cycle, CDKs and cancer: a changing paradigm. *Nat. Rev. Cancer*, **9**, 153–166.
22. Lim,Y., Lee,E., Lee,J., Oh,S. and Kim,S. (2008) Down-regulation of asymmetric arginine methylation during replicative and H2O2-induced premature senescence in WI-38 human diploid fibroblasts. *J. Biochem.*, **144**, 523–529.
23. Fujimoto,K., Matsuura,K., Hu-Wang,E., Lu,R. and Shi,Y.B. (2012) Thyroid hormone activates protein arginine methyltransferase 1 expression by directly inducing c-Myc transcription during Xenopus intestinal stem cell development. *J. Biol. Chem.*, **287**, 10039–10050.
24. Kim,D., Lee,J., Cheng,D., Li,J., Carter,C., Richie,E. and Bedford,M.T. (2010) Enzymatic activity is required for the in vivo functions of CARM1. *J. Biol. Chem.*, **285**, 1147–1152.

25. Gartel,A.L. and Shchors,K. (2003) Mechanisms of c-myc-mediated transcriptional repression of growth arrest genes. *Exp. Cell Res.*, **283**, 17–21.
26. Brenner,C., Deplus,R., Didelot,C., Loriot,A., Vire,E., De Smet,C., Gutierrez,A., Danovi,D., Bernard,D., Boon,T. *et al.* (2005) Myc represses transcription through recruitment of DNA methyltransferase corepressor. *EMBO J.*, **24**, 336–346.
27. Lanigan,F., Geraghty,J.G. and Bracken,A.P. (2011) Transcriptional regulation of cellular senescence. *Oncogene*, **30**, 2901–2911.